RESULTS FROM HERMES

Wolfgang Lorenzon*
Randall Laboratory of Physics
University of Michigan, Ann Arbor, Michigan 48109-1120
and
Deutsches Elektronen-Synchrotron, DESY, D-22603 Hamburg, Germany

Representing the HERMES Collaboration

ABSTRACT

HERMES, HERA Measurement of Spin, is an experiment to study the spin structure of the nucleon. The experiment was installed and commissioned in 1995 in the HERA storage ring at the DESY laboratory in Hamburg, Germany. Inclusive and semi-inclusive spin-dependent deep inelastic scattering on polarized internal gas targets are measured simultaneously. Data were taken on polarized ^{3}He and ^{1}H targets as well as on unpolarized targets of hydrogen, deuterium, ^{3}He, and nitrogen. The experiment is described briefly and some recent results from the 1995 to 1997 running periods are presented.

*Supported by NSF Contract PHY-9724838.

1 Introduction

Understanding how the spin of the nucleon is constructed from its elementary constituents has proven to be a significant challenge both theoretically and experimentally. In a simple parton model the spin of the nucleon can be decomposed as[1]

$$\frac{1}{2} = \frac{1}{2}\Delta\Sigma + \Delta G + \Delta L_q + \Delta L_G, \quad (1)$$

where $\Delta\Sigma$ and ΔG are the intrinsic spins carried by the quarks and gluons, and ΔL_q and ΔL_G the orbital angular momenta of the quarks and gluons. Whereas the left hand side of Eq. (1) is very well known, the right hand side has been investigated for more than twenty years, starting at SLAC in 1975. Scattering polarized leptons off polarized nucleons has been the method of choice in the past to understand the contributions to the nucleon spin from quarks. Using an analysis based on the quark parton model with QCD corrections, the main conclusion of these polarized deep inelastic scattering experiments is that the quarks contribute only at the 20% level to the nucleon's spin,[2] much lower than expected from the relativistic quark parton model. No direct measurements of the other components are available at present.

Many open questions remain: what are the contributions of the other components; what are the individual quark contributions to $\Delta\Sigma$, i.e., what is the contribution of the valence quarks, the sea quarks—in particular the strange quarks, and what is the role of the glue?

2 HERMES Experiment

HERMES has been designed[3] to address many of these open questions using a new experimental technique to measure spin-dependent deep inelastic scattering. Inclusive and semi-inclusive spin-dependent measurements are done simultaneously on undiluted polarized ^{1}H, ^{2}D, and ^{3}He targets. Semi-inclusive spin asymmetries resulting from hadron particle identification provide the means to investigate the spin structure of the nucleon in a new way. HERMES provides data not only on polarized structure functions but also on unpolarized structure function ratios, investigates the light sea flavor asymmetry, extracts information on fragmentation functions, and studies hadronization in nuclei. A sizeable program exists also in diffractive vector meson production of ρ, ϕ, ω, and J/Ψ mesons to extract cross sections, decay angular distributions, and to study nuclear transparency. HERMES also studies transversity and azimuthal distributions in polarized Λ production, etc.

The HERMES experiment is located in the east section of the HERA electron-proton collider. The experiment is arranged such that the 27.5 GeV longitudinally polarized electron beam interacts with internal polarized gas targets without interference from the proton beam. The beam is self-polarized transverse to the beam direction by emission of synchrotron radiation in the curved sections (Sokolov-Ternov effect[4]). Spin rotators located at the entrance and exit of the east straight section[5] precess the spin direction from vertical to longitudinal at the target position. The polarization builds up with a rise time of about 25 minutes and is measured with two polarimeters. Figure 1 shows a typical polarization rise time recorded by both polarimeters.

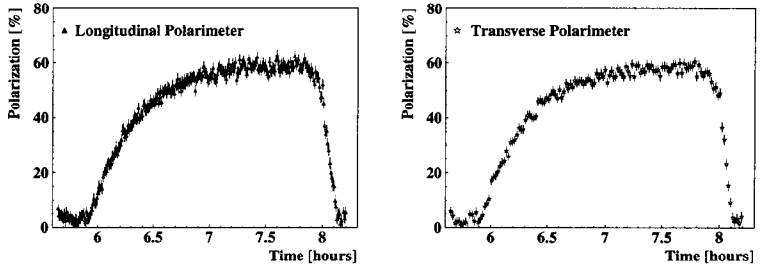

Figure 1. Polarization rise time recorded simultaneously with the longitudinal and transverse polarimeters to compare build-up time and general performance of both polarimeters. At the beginning and the end of the spectrum, the beam was depolarized on purpose.

In 1995 data were taken with a polarized ^{3}He target, and in 1996/97 HERMES was running with a polarized hydrogen target. The HERMES target[3,6] is contained in an open-ended thin walled storage cell through which the circulating electron beam of the HERA accelerator passes. The target region surrounding the storage cell is displayed schematically in Fig. 2. A magnetic holding field provides a quantization axis for the target polarization. Polarized gas enters the target cell through a central feed tube and then leaves the cell at the ends, where high speed pumps prevent the gas from flowing into the electron beam pipe. In 1995, a typical ^{3}He polarization of 50% was obtained. In 1996 and 1997, the atomic beam source had achieved hydrogen polarization of 80–95%. Unpolarized hydrogen, deuterium, ^{3}He, and nitrogen gases up to 10^{15} atoms/cm^2 have also been used to check the detectors in the spectrometer and to take

unpolarized data. The maximum target thickness is determined by the impact on the stored electron lifetime.

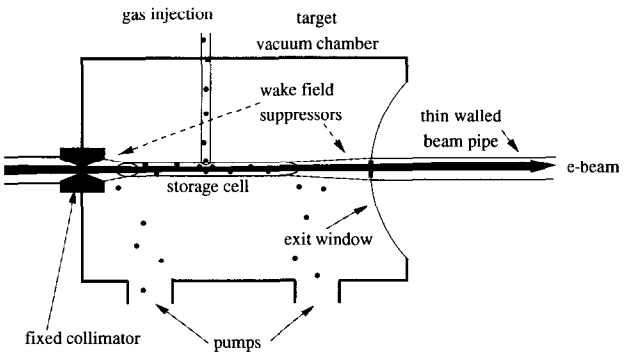

Figure 2. Schematic of the HERMES target region. See text for more explanation.

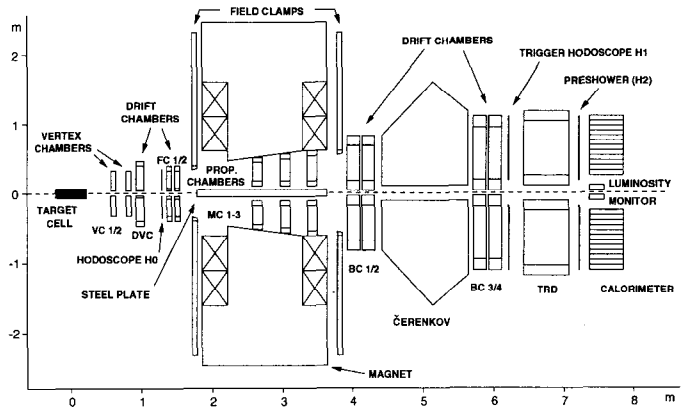

Figure 3. Schematic side view of the HERMES spectrometer.

The HERMES spectrometer, as shown in Fig. 3, was designed[3,7] to detect scattered electrons and hadrons from deep inelastic scattering. The spectrometer consists of two identical halves above and below the electron ring plane. This provides two independent measurements of observables and thus, a cross check on systematic uncertainties. The HERMES spectrometer contains a bending magnet to measure particle momenta and to reject background. Tracking chambers before the magnet, inside the magnetic field, and behind the magnet provide charged particle tracking. The Cherenkov, transition radiation detector (TRD), hodoscope (H1), and calorimeter are used for particle identification, and the magnet and calorimeter for momentum and energy analysis.

3 The Spin Structure of the Nucleon

Experimentally, the spin structure function g_1 is extracted from the measured asymmetry, $A_{\parallel}$, of the scattering cross section as the beam or target spin is flipped. These asymmetries are measured with longitudinally polarized beams and longitudinally polarized targets. Ignoring contributions from transverse asymmetries for the purpose of simplicity here, this can be written as $A_{\parallel} \approx D(x,y)A_1$, where $D(x,y)$ is the virtual photon depolarization factor and A_1 the longitudinal virtual photon asymmetry. Finally, g_1 is determined using

$$g_1(x,Q^2) = \frac{A_{\parallel}}{D}\frac{F_2(x,Q^2)}{2x(1+R(x,Q^2))}\,, \qquad (2)$$

with parametrizations of the unpolarized structure function[9] $F_2(x,Q^2)$ and $R(x,Q^2)$ (Ref. 10), the ratio of longitudinal to transverse virtual photon absorption cross sections.

The first HERMES results for the proton spin structure function[11] taken on polarized ^{1}H in 1997 are presented in Fig. 4 and compared to the published data from SLAC[12] and SMC.[8,13] The structure function ratio g_1^p/F_1^p, which is approximately equal to A_1, is given for the measured Q^2 at each value of x. There is good agreement between these three sets of data, although the Q^2 values of E-143 and HERMES differ from those of SMC by a factor between five and ten. This demonstrates that there is no statistically significant Q^2 dependence of the ratio g_1^p/F_1^p in the Q^2 range of these experiments.

In Fig. 5 the spin structure function g_1^p on the proton is shown as a function of x, evolved to a common Q^2 of 2 and 10 GeV^2 for comparison with the SLAC and SMC results. The evolution was done under the assumption that the ratio g_1^p/F_1^p does not depend on Q^2. The evolved HERMES data are in excellent agreement with both data sets. The apparent Q^2 dependence of g_1^p, seen when comparing the left and right plots, entirely originates from the Q^2 dependence of F_2^p and R. In summary, the HERMES results were obtained using an entirely different technique from that used in all previous experiments, indicating that the systematic uncertainties are well understood for both techniques over the entire measured x range.

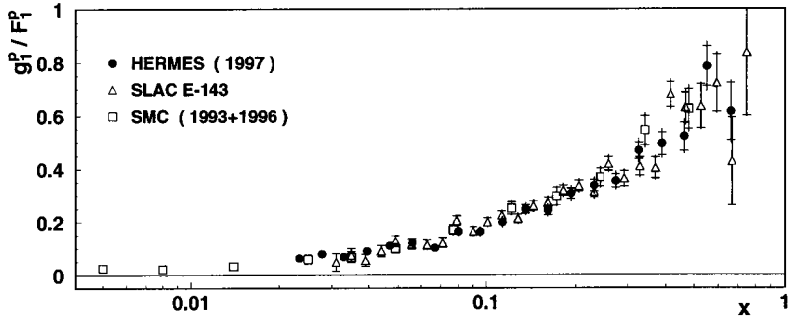

Figure 4. The structure function ratio g_1^p/F_1^p of the proton as a function of x from HERMES is compared with recent results for g_1^p/F_1^p measured at SLAC (E143) and A_1^p at CERN (SMC). The inner error bars show the statistical uncertainties and the outer ones the quadratic sum of the statistical and total systematic uncertainties.

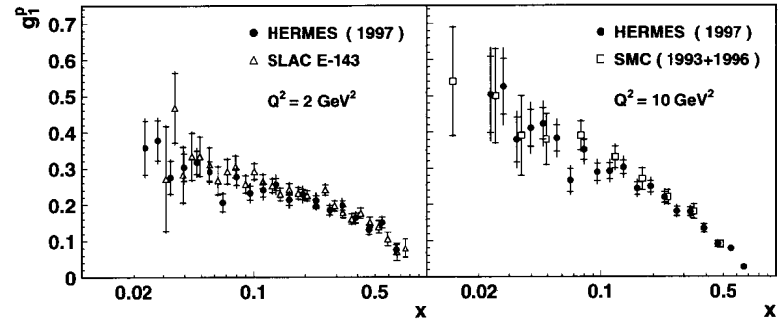

Figure 5. The spin structure function g_1^p on the proton is shown as a function of x. In the left panel, the HERMES data are evolved to $Q^2 = 2$ GeV^2 and compared to recent results for $Q^2 > 1$ GeV^2 from E143 (Ref. 12). In the right panel, the HERMES data are evolved to $Q^2 = 10$ GeV^2 and compared to recent results for $Q^2 > 1$ GeV^2 and $x > 0.01$ from SMC (Ref. 13). The error bars are defined as in Fig. 4.

A summary of spin structure function measurements is shown in Table 1, where the beams, targets, energies, and measured quantities are listed for each experiment. The experiments complement each other in their kinematic coverage and their sensitivities to possible systematic errors associated with the measured quantities. The pioneering

Table 1. Summary of experiments at SLAC, CERN, and DESY to measure spin-dependent deep inelastic scattering.

Lab	Experiment	Year	Beam	Target	Measured Quantities
SLAC	E80	75	23 GeV e^-	H–butanol	A_1^p
	E130	80	23 GeV e^-	H–butanol	A_1^p
	E142	92	25 GeV e^-	^{3}He	A_1^n
	E143	93	29 GeV e^-	NH_3/ND_3	A_1^p,A_1^d,$A_2^{p,d}$
	E154	95	49 GeV e^-	^{3}He	A_1^n, A_2^n
	E155	97	49 GeV e^-	NH_3/LiD	A_1^p,A_1^d
CERN	EMC	85	100-200 GeV μ^-	NH_3	A_1^p
	SMC	92	100 GeV μ^+	D–butanol	A_1^d,$A_{1,h}^d$
	SMC	93	190 GeV μ^+	H–butanol	A_1^p,$A_{1,h}^p$
	SMC	94/95	190 GeV μ^+	D–butanol	A_1^d,$A_{1,h}^d$
	SMC	96	190 GeV μ^+	NH_3	A_1^p,$A_{1,h}^p$
DESY	HERMES	95	28 GeV e^+	^{3}He	A_1^n, $A_{1,h}^n$, $A_{\perp,\pi}^n$
	HERMES	96/97	28 GeV e^+	^{1}H	A_1^p, $A_{1,h}^p$, $A_{1,\pi}^p$

experiments on the proton were performed at SLAC[14] with modest polarizations of beam and target. They were followed by more precise proton data from EMC[15] which, while consistent with the SLAC data, showed a large deviation from the Ellis-Jaffe sum rule[16] and a corresponding small value for the implied quark contribution to the proton's spin. This result spurred a new generation of experiments at SLAC, CERN, and DESY with significant improvements in precision.

The new experiments at SLAC, CERN, and DESY over the last six years have focused on high precision measurements of the structure function g_1 over a large kinematic range to extract information on the spin structure. They appear to be consistent if they are evolved to the same Q^2. The experiments confirmed EMC's initial observation of the violation of the Ellis-Jaffe sum rule. The Bjorken sum rule,[17] on the other hand, is verified at the 1 σ (8%) level and is considered a successful test of QCD on spin observables. They however indicate that only about 20% of the spin comes from the spin of the quarks. Therefore, the question of how the spin of the nucleon is related to its internal structure is not resolved. The need for measurements of other observables using more sophisticated experimental techniques is evident: g_1 needs to be measured at very small x; the polarization of the sea, in particular the polarization of the strange

quarks using flavor decomposition, needs to be measured; and a direct measurement of the gluon helicity distribution ΔG is important to make definitive statements about the nucleon's spin structure.

4 Semi-Inclusive Physics

To this end, HERMES is currently running a broad scope of semi-inclusive measurements. This is done by measuring the hadronic reaction products in coincidence with the scattered lepton. As shown schematically in Fig. 6, it should be possible in appropriate kinematics to tag the flavor of the struck quark[18] which is reflected by the type of hadron in the current jet. In this way the right hand side of Eq. (1) may be decomposed.

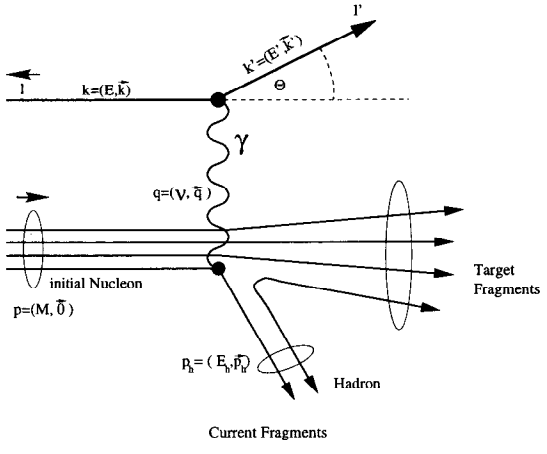

Figure 6. A schematic illustration of the hadronization process.

4.1 Flavor Tagging

Assuming factorization between the hard scattering process and the hadronization of the struck quark, the hadron asymmetry can be expressed as

$$A_1^h(x,z) \simeq \frac{A_{||}^h(x,z)}{D(x,Q^2)} \simeq \frac{\sum e_f^2 \Delta q_f(x) \cdot D_{q_f}^h(z)}{\sum e_f^2 q_f(x) \cdot D_{q_f}^h(z)}. \quad (3)$$

This equation differs from the inclusive formula by the factor $D_{q_f}^h(z)$, which represents the probability for a struck quark of flavor f to fragment into a hadron of type h with energy fraction of the virtual photon $z = E_h/\nu$. A measurement of the hadron asymmetry will then give access to new linear combinations of polarized quark distributions Δq.

Of course, the hadronization is a statistical process, and a quark with flavor f may produce either a leading π^+ or π^-. However, because of the valence quark structure of mesons, the probabilities are not equal and one can define both *favored* and *disfavored* fragmentation functions, D^+ and D^-, respectively. These pion fragmentation functions, as extracted from the HERMES data using the EMC extraction method, are shown in Fig. 7. They are compared to the EMC data.[19] There is good agreement between these two data sets.

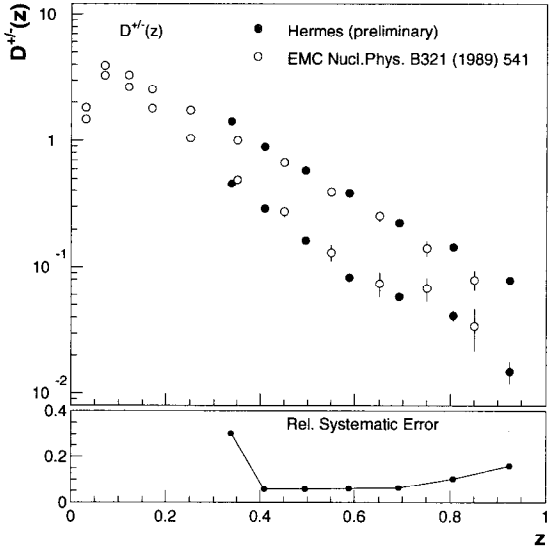

Figure 7. Preliminary data on the favored D^+ and disfavored D^- pion fragmentation functions from HERMES are compared to data from EMC. They are shown in the top panel. The same extraction method has been used for both data sets. The relative systematic errors are displayed in the lower panel.

Figure 8 displays the hadron asymmetries measured in 1995 on polarized ^{3}He and in 1996 on polarized ^{1}H targets. In the top panel the inclusive asymmetry A_1^p, and the semi-inclusive asymmetries for positive $A_1^p(h^+)$ and negative $A_1^p(h^-)$ hadrons on proton targets are shown. The corresponding asymmetries on ^{3}He are shown in the

bottom panel. The semi-inclusive asymmetries are compared to the available SMC semi-inclusive data.[20] There is generally good agreement between the two data sets.

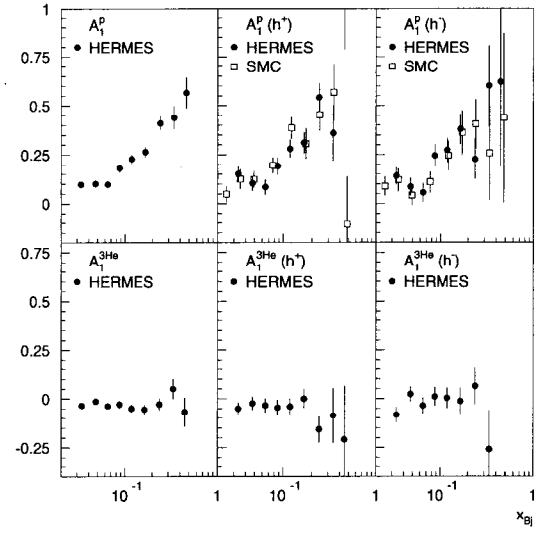

Figure 8. Preliminary data for positive and negative charged hadron asymmetries on the proton and ^{3}He from HERMES are compared to available data from the SMC experiment. Also included are the inclusive asymmetries on the proton and ^{3}He from HERMES for comparison.

In order to extract the polarized quark distributions, several quantities are needed[21] as input: the measured hadron asymmetries $A_1^h(x,z)$, the unpolarized quark distributions $q(x)$, and the fragmentation functions $D_{q_f}^h(z)$. It is further necessary to rewrite the photon-nucleon asymmetry (Eq. (3)) in such a way that one can isolate the quark polarizations, and end up with a sum over quark purities times the quark polarizations:

$$A_1^h(x,z) = \sum_q \frac{e_q^2 q(x) D_q^h(z)}{\sum_{q'} e_{q'}^2 q'(x) D_{q'}^h(z)} \cdot \frac{\Delta q(x)}{q(x)} = \sum_q P_q^h(x,z) \cdot \frac{\Delta q(x)}{q(x)}. \quad (4)$$

The quark purity P_q^h is the conditional probability that a quark q was struck in an event, if a hadron of type h was produced. The purities are spin-independent, unpolarized quantities. They are produced by Monte Carlo simulations tuned using unpolarized HERMES hadron multiplicities. A matrix equation including various hadron asymmetries and quark polarizations can then be defined as

$$\vec{A} = \mathcal{P}\vec{\mathcal{Q}}. \quad (5)$$

To extract the quark polarizations this matrix equation has to be solved.

Since the sea purities are too small for decomposition with the statistics that is currently available, it is assumed that the relative polarization of the sea quarks is flavor symmetric,

$$\frac{\Delta u_{sea}}{u_{sea}} = \frac{\Delta d_{sea}}{d_{sea}} = \frac{\Delta s}{s}, \quad (6)$$

to reduce the number of degrees of freedom. It is then possible to extract the polarizations of the u-valence, d-valence, and sea quarks. In order to compare with the data from SMC,[20] x times the polarized quark distributions are plotted in Fig. 9.

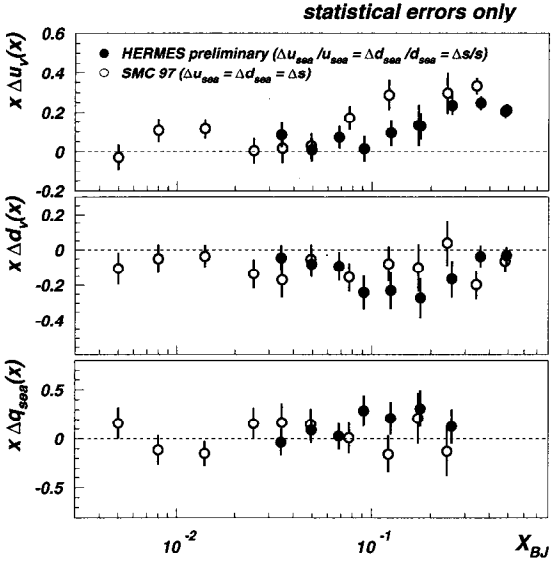

Figure 9. Preliminary data on the quark spin distributions at the measured Q^2 are shown separately for the valence Δu_v, Δd_v, and the sea $\Delta\bar{u}$ as a function of x. The error bars shown are statistical only. The distributions are compared to results from SMC evolved to $Q^2 = 10$ GeV^2. The error bars of the SMC result correspond to its total uncertainty.

Note, that even though different sea quark assumptions are used for HERMES (equal polarizations) and SMC (SU(3) flavor symmetric sea), the results change by less than 10%. The SMC results, evolved to a fixed Q^2 of 10 GeV^2, are in rough agreement with the polarized quark distributions at HERMES, which are given at their measured Q^2.

4.2 Unpolarized Semi-Inclusive Results

As with polarized scattering, flavor tagging with unpolarized targets allows flavor dependent separation of valence and sea quark probability densities. By forming the ratio of charged pion yields on ^{1}H and ^{2}D targets,

$$r(x,z) = \frac{N_p^{\pi^-}(x,z) - N_n^{\pi^-}(x,z)}{N_p^{\pi^+}(x,z) - N_n^{\pi^+}(x,z)}, \qquad (7)$$

one can extract the flavor content of the nucleon sea. Here $N^\pi(x,z)$ is the yield of pions coming from deep inelastic scattering off nucleons. Until recently, there has been little experimental constraint on the flavor asymmetry in the distributions of the light sea quarks in the nucleon. The first one was an integral test, based on a comparison of inclusive deep inelastic scattering on the proton and the neutron to determine the Gottfried sum[22] defined as $S_G = \int_0^1 \frac{dx}{x}(F_2^p(x) - F_2^n(x))$, where $F_2^p(x)$ and $F_2^n(x)$ are the structure functions of the proton and neutron, respectively. The assumption of isospin symmetry in the quark parton model allows the sum to be written as $S_G = \frac{1}{3} - \frac{2}{3}\int_0^1(\bar{d}(x) - \bar{u}(x))dx$. A flavor symmetric sea, $\bar{d}(x) = \bar{u}(x)$, leads to the Gottfried Sum Rule $S_G = 1/3$. A measurement by NMC[23] resulted in $S_G = 0.235 \pm 0.026$. If isospin symmetry holds, a global flavor asymmetry $\int_0^1(\bar{d}(x) - \bar{u}(x))dx \approx 0.15$ would account for the NMC result. Two methods have been proposed to measure its x dependence: The Drell-Yan process[24] and semi-inclusive deep inelastic scattering.[25] HERMES can measure the ratio $(\bar{d} - \bar{u})/(u - d)$ from the ratio of charged pion yields defined in Eq. (7), in semi-inclusive DIS on ^{1}H and ^{2}D.

Results[26] are presented for the x dependence of $(\bar{d} - \bar{u})/(u - d)$ in Fig. 10. Within the measured x region, the values are nonzero and positive everywhere, clearly showing an excess of $\bar{d}$ quarks over $\bar{u}$ quarks in the proton. Note that no higher order QCD corrections have been made and so only leading order parametrizations should be compared to these results. At low Q^2, only GRV 94 LO[27] is available at leading order. The distribution $\bar{d} - \bar{u}$ as a function of x is thus derived from $(\bar{d} - \bar{u})/(u - d)$ using the GRV 94 LO parametrization of $u_v(x) - d_v(x)$. The alternative approach to the measurement of the flavor asymmetry is the comparison of the Drell-Yan process on protons and deuterons, which is sensitive to the quantity $\bar{u}/\bar{d}$. The E866 collaboration at Fermilab recently reported a measurement of the flavor asymmetry[31] using the CTEQ 4M parametrization of $\bar{u} + \bar{d}$ to extract $(\bar{d} - \bar{u})$ from the measured quantity $\bar{u}/\bar{d}$. These results at Q^2 of 54 GeV^2 are included in the lower plot. This figure demonstrates that the sea asymmetry measured in deep inelastic scattering and in Drell-Yan experiments agree, even though the Q^2 of the two experiments differ by a factor of about 20.

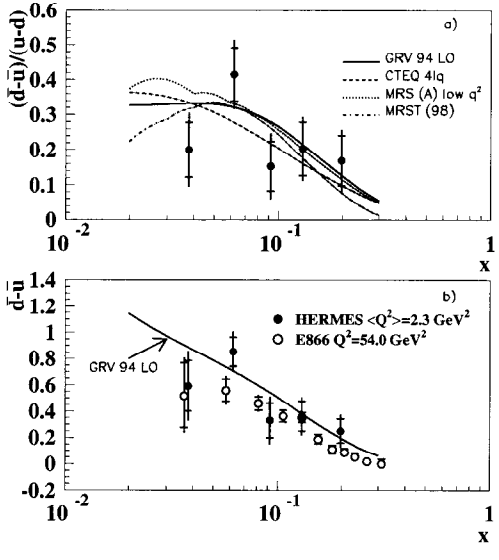

Figure 10. In the top panel, $(\bar{d} - \bar{u})/(u - d)$ as a function of x is shown. Also included are GRV 94 LO (Ref. 27), CTEQ 4lq (Ref. 28), MRS (A) low Q^2 (Ref. 29), and MRST (98) (Ref. 30) parametrizations calculated at the appropriate Q^2 for each x-bin. In the bottom panel $(\bar{d}$-$\bar{u})$ as a function of x is shown. The curve is the GRV 94 LO parameterization. The E866 data determined from $(\bar{d}$-$\bar{u})$ are represented by open circles.

5 Future

At present, no direct measurement of the gluon contribution to the nucelon's spin is available. While NLO analyses of the inclusive data suggest that the gluon carries a

significant fraction of the nucleon spin[32-36] to compensate the deficit due to the intrinsic quark distribution, it is clear that a direct measurement of the gluon spin contribution is very important. Several experimental efforts are underway to measure spin-dependent charm production which should probe the gluons via the photon-gluon fusion reaction. These include the COMPASS experiment at CERN (Ref. 37), the SLAC proposal E156 (Ref. 38), and the HERMES experiment at DESY. The HERMES collaboration has just finished an upgrade of the spectrometer to enhance kaon identification using a Ring Imaging Cherenkov (RICH) counter to probe the strange sea, and to enhance charm identification to probe the gluon spin (Ref. 39). In addition, the RHIC (Ref.40) experiments at BNL plan to probe the gluon spin by direct photon production. Further, it has been shown that HERA, with polarized protons in collider mode and with significantly increased luminosity, can probe gluon spin at low x (Ref. 41). Table 2 summarizes the likely sensitivities of these experiments. The upgrade of the HERMES spectrometer could provide direct information on the sign of the gluon polarization by about 2000. The planned experiments at CERN, RHIC, and SLAC should be able to provide significantly more precise information in the early years of the next decade.

Table 2. Summary of experiments at BNL, CERN, SLAC, and DESY to directly probe gluon spin.

Experiment	Results expected by	Kinematic range	$\delta\left(\frac{\Delta G}{G}\right)$
HERMES	1999	$x_g \sim 0.3$	~ 0.5 /year
RHIC	$\sim 2001/2$	$x_g \sim 0.05 - 0.3$	$\sim 0.01 - 0.3$
COMPASS	$\sim 2002/3$	$x_g \sim 0.15$	~ 0.1
SLAC E-156	deferred	$x_g \sim 0.1 - 0.5$	~ 0.02
pol. HERA	not approved	$x_g \sim 0.01 - 0.1$	~ 0.1

6 Conclusions

The HERMES experiment has successfully finished its third year of data taking. Inclusive and semi-inclusive data are collected simultaneously using polarized internal gas targets. This novel target technology has proven to work well and has provided competitive results with different systematic errors than the previous experiments. The recent upgrades to the spectrometer have opened new possibilities for HERMES. It is expected that by the end of 1999, HERMES will provide precise knowledge of the valence and sea quark polarizations, report on the first direct measurement of the strange quark polarization, and maybe make the first direct measurement of the gluon polarization.

7 Acknowledgements

I wish to thank my colleagues in the HERMES collaboration. I acknowledge C. A. Miller for critical reading of the manuscript. The author's research is supported in part by the U. S. National Science Foundation, Nuclear Physics Division under grant No. PHY-9724838. I thank the University of Michigan and DESY for support while on research leave.

References

[1] R. L. Jaffe and A. Manohar, Nucl. Phys. B **337**, 509 (1990).

[2] D. Adams *et al.*, Phys. Lett. B **357**, 248 (1995).

[3] HERMES Collaboration, Technical Design Report, DESY-PRC 93/06 (1993).

[4] A. A. Sokolov and I. M. Ternov, Sov. Phys. Dokl. **8**, 1203 (1964).

[5] J. Buon and K. Steffen, Nucl. Instrum. Methods A **245**, 248 (1986).

[6] F. Stock *et al.*, Nucl. Instrum. Methods A **343**, 334 (1994); L. H. Kramer *et al.*, Nucl. Instrum. Methods A **365**, 49 (1995).

[7] K. Ackerstaff *et al.*, Nucl. Instrum. Methods A **417**, 230 (1998).

[8] D. Adams *et al.*, Phys. Lett. B **336**, 125 (1994).

[9] M. Arneodo *et al.*, Phys. Lett. B **364**, 107 (1995).

[10] L. W. Whitlow *et al.*, Phys. Lett. B **250**, 193 (1990).

[11] A. Airapetian *et al.*, Phys. Lett. B **442**, 484 (1998).

[12] K. Abe *et al.*, Phys. Rev. Lett. **74**, 346 (1995); Phys. Lett. B **364**, 61 (1995); Phys. Rev. D **58**, 112003 (1998).

[13] D. Adams *et al.*, Phys. Rev. D **56**, 5330 (1997); B. Adeva *et al.*, Phys. Lett. B **412**, 414 (1997).

[14] M. J. Alguard *et al.*, Phys. Rev. Lett. **37**, 1261 (1976); *ibid.* **41**, 70 (1978).

[15] J. Ashman *et al.*, Phys. Lett. B **206**, 364 (1988); Nucl. Phys. B **328**, 1 (1989).

[16] J. Ellis and R. L. Jaffe, Phys. Rev. D **9**, 1444 (1974); *ibid.* **10**, 1669 (1974).

[17] J. D. Bjorken, Phys. Rev. **148**, 1467 (1966); Phys. Rev. D **1**, 1376 (1970).

[18] J. M. Niczyporuk and E. E. W. Bruins, Phys. Rev. D **58**, 091501 (1998).

[19] M. Arneodo *et al.*, Nucl. Phys. B **321**, 541 (1989).

[20] B. Adeva *et al.*, Phys. Lett. B **420**, 180 (1998).

[21] M. A. Funk, "A Measurement of the Polarized Parton Densities of the Nucleon in Deep-Inelastic Scattering at HERMES," Ph.D. thesis, University of Hamburg, DESY-Thesis-1998-017, (1998) unpublished.

[22] K. Gottfried, Phys. Rev. Lett. **18**, 1174 (1967).

[23] M. Arneodo *et al.*, Phys. Rev. D **50**, 1 (1994).

[24] S. D. Ellis and W. J. Stirling, Phys. Lett. B **256**, 258 (1991).

[25] J. Levelt *et al.*, Phys. Lett. B **263**, 498 (1991).

[26] K. Ackerstaff *et al.*, Phys. Rev. Lett. **81**, 5519 (1998).

[27] M. Glück *et al.*, Z. Phys. C **67**, 433 (1995).

[28] H. L. Lai *et al.*, Phys. Rev. D **55**, 1280 (1997).

[29] A. D. Martin *et al.*, Phys. Rev. D **51**, 4756 (1995).

[30] A. D. Martin *et al.*, Eur. Phys. J. C **4**, 463 (1998).

[31] E. A. Hawker *et al.*, Phys. Rev. Lett. **80**, 3715 (1998); J. C. Peng *et al.*, Phys. Rev. D **58**, 092004 (1998).

[32] J. Ellis and M. Karliner, Phys. Lett. B **341**, 397 (1995).

[33] R. D. Ball, S. Forte, and G. Ridolfi, Phys. Lett. B **378**, 255 (1996).

[34] M. Glück, E. Reya, M. Stratmann, and W. Vogelsang, Phys. Rev. D **53**, 4775 (1996).

[35] T. Gehrmann and W. S. Stirling, Phys. Rev. D **53**, 6100 (1996).

[36] G. Altarelli *et al.*, Nucl. Phys. B **496**, 337 (1997).

[37] COMPASS Proposal, CERN/SPSLC-96-14 (1996).

[38] SLAC Proposal E156, March 15, 1997.

[39] M. Amarian *et al.*, HERMES Report 97-004, "The HERMES Charm Upgrade Program," January 24, 1997.

[40] G. Bunce *et al.*, Particle World **3**, 1 (1992).

[41] A. De Roeck *et al., Proceedings of the Workshop on Future Physics at HERA* 1995/96, Volume 2, page 803, September 1996.